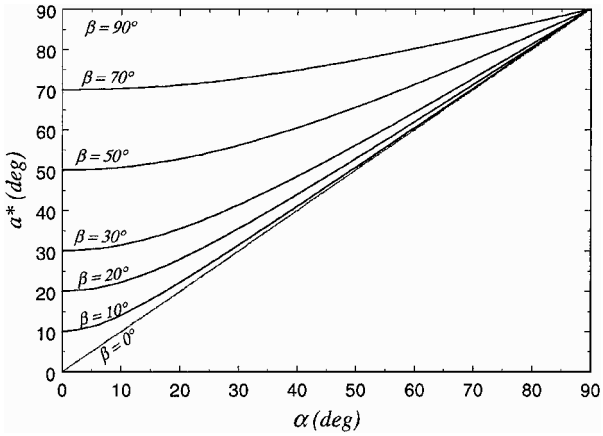

Fig. 2 Equivalent angles of attack in orientations with pure sideslip and pure roll.

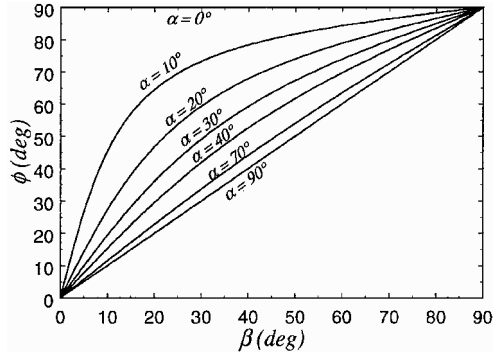

Fig. 3 Equivalent roll and sideslip angles.

From simple geometric considerations (Fig. 1), one may derive the expressions

$$u = V \cos\beta \cos\alpha \tag{4}$$

$$w = V \cos\beta \sin\alpha \tag{5}$$

$$v = V \sin a^* \sin\varphi \tag{6}$$

$$w = V \sin a^* \cos\varphi \tag{7}$$

From Eqs. (3) and (4), one gets a relationship between the equivalent angles of attack as

$$a^* = \cos^{-1}(\cos\beta \cos\alpha) \tag{8}$$

Further equating the ratios v/w obtained by combining Eqs. (2) and (5) and Eqs. (6) and (7), one gets a relationship between the equivalent roll and sideslip angles as

$$\varphi = \tan^{-1}(\tan\beta / \sin\alpha) \tag{9}$$

The equivalent angle α^* has been plotted vs α for different values of β in Fig. 2. It is obvious that, when $\beta = 0$, then $\alpha = a^*$, whereas when $\alpha = 0$, then $\alpha^* = \beta$. For small β (typically, for $\beta < 5$ deg), $\alpha \approx \alpha^*$, but, otherwise, there is a significant difference between α and α^*. The equivalent φ has been plotted vs β for different values of α in Fig. 3. Clearly, $\varphi = 90$ deg, when $\alpha = 0$, and $\varphi = \beta$, when $\alpha = 90$ deg. For small β (typically, for $\beta < 5$ deg), $\varphi \approx \beta / \sin\alpha$, for example, $\varphi \approx \frac{1}{2}\beta$, for $\alpha = 30$ deg.

Conclusions

The described method permits the conversion of wind-tunnel results obtained by angle-of-attack/sideslip-angle combinations into equivalent roll results. If applied at an early stage of planning, the same approach provides guidance for the design of the simplest model mounting system that would permit the model orientation within the desired range.

Acknowledgment

The author acknowledges the financial support of the Institute for Aerospace Research, National Research Council of Canada, and the useful discussions with B. H. K. Lee and X. Z. Huang.

References

[1]Etkin, B., *Dynamics of Atmospheric Flight*, Wiley, New York, 1972, Chap. 4.3, p. 114.

[2]Wright, J., *A Compilation of Aerodynamic Nomenclature and Axes Systems*, United States Naval Ordnance Lab., NOLR 1241, White Oak, Silver Spring, MD, 1962, pp. 1–93.

Acceleration Effect on the Stanton Number for Castings of Ice-Roughened Surfaces

Nihad Dukhan,* K. C. Masiulaniec,† and Kenneth J. De Witt‡
University of Toledo, Toledo, Ohio 43606
and
G. James Van Fossen Jr.§
NASA John H. Glenn Research Center at Lewis Field, Cleveland, Ohio 44135

Introduction

A PREVIOUS study[1] provided fundamental information on the effect of surface roughness, due to ice accretion, on the surface rate of heat transfer for parallel flow over aluminum castings of stochastically accreted ice. The roughness enhanced the heat transfer rate and lowered the Reynolds number for the onset of transition to turbulent flow as compared to the smooth model case. The Stanton numbers were higher than those obtained with the uniform roughness elements of other studies.[2,3] The current study was conducted to provide characteristics of the convective heat transfer from stochastically accreted ice-roughened surfaces, described in Ref. 1, in accelerated flows. These data are needed for the effective sizing and design of in-flight de-icing systems.

Few previous studies have included the effect of acceleration on the rate of heat transfer from rough surfaces. Coleman[4] stated that flow acceleration increased the heat transfer rate in the fully rough regime, and Poinsatte et al.[5] reported that varying the angle of attack for an artificially roughened airfoil caused heat transfer to increase over the 0-deg case.

Heat transfer data for the smooth flat plate model and for each of the seven roughness models described in Ref. 1 were collected for the approach velocities of $u_\infty = 9.4, 20.7$, and 32.6 m/s at inclination angles of $\theta = 5$, 14, 23, and 41 deg. This Note presents complete results for the smooth model at $u_\infty = 32.6$ m/s and roughness model

Presented as Paper 96-0867 at the AIAA 34th Aerospace Sciences Meeting, Reno, NV, 15–19 January 1996; received 7 April 1998; revision received 22 March 1999; accepted for publication 23 March 1999.

*Graduate Student, Department of Mechanical, Industrial and Manufacturing Engineering; currently Senior Engineer, RELTEC Corporation, 4350 Weaver Parkway, Warrenville, IL 60555-3930.

†Associate Professor, Department of Mechanical, Industrial and Manufacturing Engineering.

‡Professor, Department of Chemical Engineering.

§Senior Research Scientist, Turbomachinery and Propulsion Systems Division.

data at the same freestream velocity for inclination angles of 14 and 41 deg. Complete results are available in the work by Dukhan.[6]

To obtain the cited inclination angles in the wind tunnel, it was necessary to adjust the angle of the saddle holding the test plate. This caused the leading edge of the model to be lowered, which resulted in a cross-sectional flow area that was larger at the model leading edge than for the parallel flow case in Ref. 1. This area then decreased with model length and was less at the trailing edge than for the parallel flow cases. Correspondingly, the freestream velocity along each model was different from the approach velocity, being lower at the leading edge and higher near the trailing edge. The ratio of the freestream velocity $u_{\infty,x}$ to the approach velocity u_∞ was obtained as a function of distance from the leading edge of the smooth plate. The ratio of these two velocities varied from 0.9 at the leading edge to 1.1 at the trailing edge for the 5-deg case. For the higher inclination angles of 14, 23, and 41 deg, the corresponding ratio variations were $\frac{0.6}{1.1}$, $\frac{0.5}{1.2}$, and $\frac{0.3}{1.5}$, respectively. The experimental procedures and data reduction techniques used are identical to those of the parallel flow study.[1]

Smooth Model Results

Figure 1 shows the Stanton number curves for the smooth model for an approach velocity of 32.6 m/s and all inclination angles. The local Reynolds number on the abscissa is based on the axial location on the model, as well as on the freestream velocity $u_{\infty,x}$ discussed earlier. The data for the 5-deg angle was almost identical to the parallel plate or 0-deg Stanton number results in Ref. 1. For Reynolds numbers up to 2.5×10^5, a slight decrease of the rate of heat transfer with increasing angle is noticed. The experimental Stanton numbers then show an opposite behavior with inclination angle (except for the $\theta = 14$ deg case) until transition occurs at approximately $Re_x = 7 \times 10^5$ for all cases. In the transitional region, the Stanton number curves for the angles of $\theta = 14$ and 23 deg are lower than for the 5-deg case. This is in agreement with the observation made by Keller[7] that mild acceleration slows the transition rate by damping the cross-stream fluctuations, and with Schlichting,[8] who, using stability theory, predicted that acceleration would have a stabilizing effect. The highly accelerated case, $\theta = 41$ deg, has a somewhat higher Stanton number, but the values are still lower than those for the 5-deg case for the same local Reynolds number.

Thus, the smooth plate results show that increasing inclination angle first decreases and then increases the heat transfer rate as compared with the parallel flow case before transition begins. After transition, increasing angles lower the rate of transition, resulting in lower Stanton numbers than for the parallel flow case.

Also shown in Fig. 1 are Kays's[9] integral and Schlichting's[8] wedge solutions for the convective heat transfer rate from a smooth 41-deg inclined surface. The velocities used for each calculation are the freestream values. Schlichting's[8] solution agrees with the present values up to about $Re_x = 3 \times 10^5$, after which it predicts lower values. Kays's[9] solution predicts lower values for all Reynolds numbers. Neither solution has the capability to predict transition.

Roughness Models Results

Figure 2 is a composite plot of the Stanton number vs the local Reynolds number, again based on the freestream velocity and the axial position, for all seven roughness models at $\theta = 14$ deg and a constant approach velocity of 32.6 m/s. For $Re_x < 2.4 \times 10^5$, the roughness height $\bar{H}$ influences the rate of heat transfer. The Stanton numbers, with some overlap, increase with $\bar{H}$, beginning with roughness model 6 (smooth glaze), then roughness model 5 (closely spaced rime ice), then model 7 (smooth rime), followed by models 1, 2, and 3 (closely spaced, loosely spaced, and intermediately spaced rough glaze, respectively), and finally roughness model 4 (rime feathers). For $Re_x > 2.4 \times 10^5$, this dependence on $\bar{H}$ is no longer clearly evident. Similar to the parallel flow case, the fully turbulent regime is present for roughness models 1–4 and 7, whereas roughness models 5 and 6 show transition beginning at

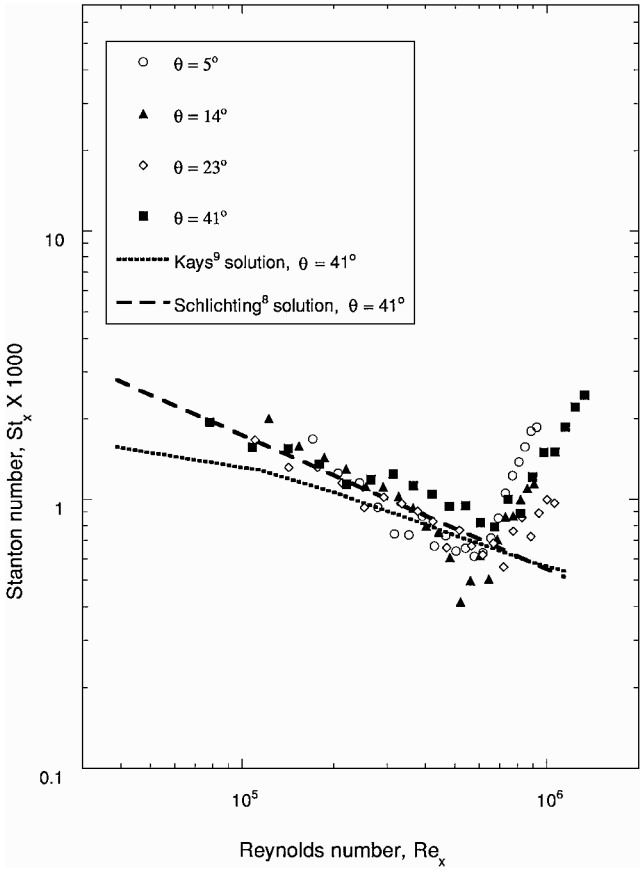

Fig. 1 Stanton number vs Reynolds number: smooth model at u_∞ = 32.6 m/s and different angles.

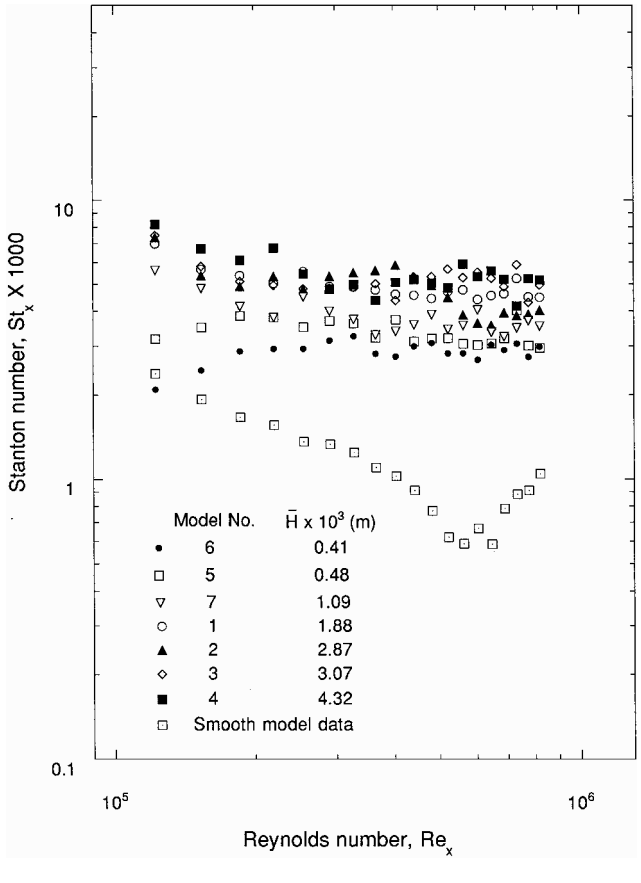

Fig. 2 Stanton number vs Reynolds number: comparison of the roughness models at u_∞ = 32.6 m/s and θ = 14 deg.

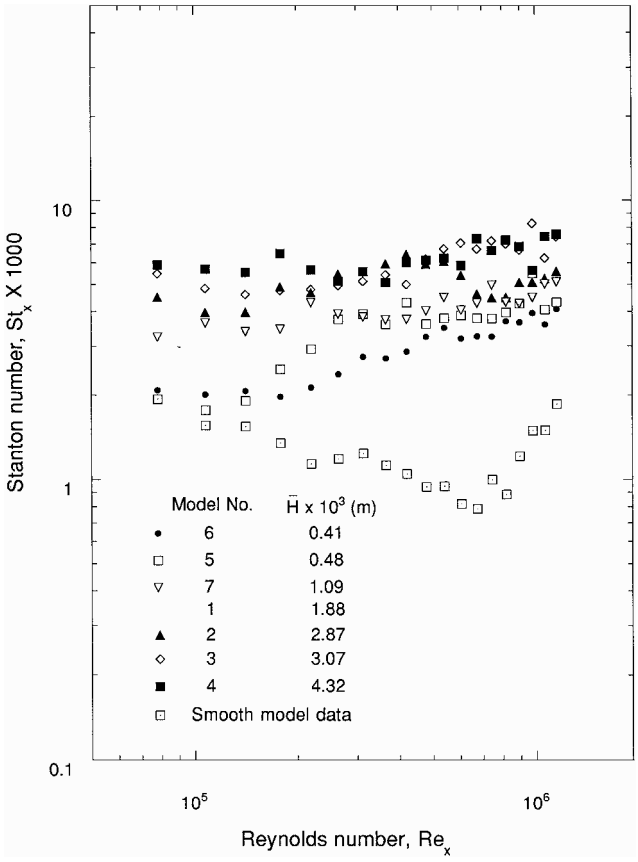

Fig. 3 Stanton number vs Reynolds number: comparison of the roughness models at u_∞ = 32.6 m/s and θ = 41 deg.

approximately $Re_x = 1.2 \times 10^5$ and are fully turbulent at approximately $Re_x = 3.5 \times 10^5$.

Figure 3 is for the high-acceleration case of 41 deg with a Reynolds number again based on the freestream velocity and local axial position. The data for roughness model 1 at this angle was lost in the processing phase. The behavior of the remaining models is similar to Fig. 2, with the Stanton numbers increasing with increasing $\bar{H}$ up to $Re_x = 2.4 \times 10^5$ and with an overlapping in the data for models 2–4 occurring for higher Reynolds numbers. The Stanton numbers are higher than in Fig. 2, and there is a wider spacing between the curves. Transition begins for models 5 and 6 at approximately $Re_x = 2.0 \times 10^5$ (a delay from the case in Fig. 2), and there is no apparent evolution toward an asymptotic state as the Stanton numbers continue to increase.

A complete set of the smooth and rough model data for the accelerated cases are available in the work by Dukhan.[6]

Conclusions

Stanton number results were obtained for the rate of convective heat transfer from aluminum castings of ice-roughened surfaces in accelerated flow. Seven models representing different types of ice accretions were tested in a wind tunnel for free-stream velocities of 9.4, 20.7, and 32.6 m/s and at inclination angles of 5, 14, 23, and 41 deg. For the smooth model, acceleration angle in general lowered the heat transfer rate before transition and delayed the onset of transition as compared to the 0-deg case. For the roughened models, the heat transfer rates for Reynolds numbers up to $Re_x = 2.4 \times 10^5$ were proportional to the roughness element height of the model, after which overlapping occurred in the data for the higher roughness element models. This was behavior similar to the parallel flow data in Ref. 1.

Acknowledgment

This effort was funded under Grant NAG 3-72 by the NASA John H. Glenn Research Center at Lewis Field, Cleveland, Ohio.

References

[1]Dukhan, N., Masiulaniec, K. C., De Witt, K. J., and Van Fossen, G. J., "Experimental Heat Transfer Coefficients from Ice-Roughened Surfaces for Aircraft Deicing Design," *Journal of Aircraft* (to be published).

[2]Hosni, M. H., Coleman, H. W., and Taylor, R. P., "Measurement and Calculations of Rough Wall Heat Transfer in the Turbulent Boundary Layer," *International Journal of Heat and Mass Transfer*, Vol. 34, No. 4, 1991, pp. 1067–1082.

[3]Hosni, M. H., Coleman, H. W., and Garner, J. W., "Roughness Shape Effect on Heat Transfer and Skin Friction in Rough-Wall Turbulent Boundary Layer," *International Journal of Heat and Mass Transfer*, Vol. 36, No. 1, 1993, pp. 147–153.

[4]Coleman, H. W., "Momentum and Energy Transport in the Accelerated Fully Rough Turbulent Boundary Layer," Ph.D. Dissertation, Dept. of Mechanical Engineering, Stanford Univ., Stanford, CA, March 1976.

[5]Poinsatte, P. E., Van Fossen, G. J., and De Witt, K. J., "Roughness Effect on Heat Transfer from a NACA 0012 Airfoil," *Journal of Aircraft*, Vol. 28, No. 12, 1991, pp. 908–911.

[6]Dukhan, N., "Measurements of the Convective Heat Transfer Coefficient from Ice Roughened Surfaces in Parallel and Accelerated Flows," Ph.D. Dissertation, Dept. of Mechanical, Industrial and Manufacturing Engineering, Univ. of Toledo, Toledo, OH, Dec. 1996.

[7]Keller, F. J., "Flow and Thermal Structure in Heated Transitional Boundary Layers with and Without Stream-Wise Acceleration," Ph.D. Dissertation, Clemson Univ., Clemson, SC, Aug. 1993.

[8]Schlichting, H., *Boundary-Layer Theory,* 7th ed., McGraw–Hill, New York, 1987, pp. 489–496.

[9]Kays, W. M., *Convective Heat and Mass Transfer,* McGraw–Hill, New York, 1966, pp. 214–226.

Unified Model Deformation and Flow Transition Measurements

Alpheus W. Burner*
NASA Langley Research Center,
Hampton, Virginia 23681-2199
Tianshu Liu† and Sanjay Garg†
High Technology Corporation, Hampton, Virginia 23666
and
James H. Bell‡ and Daniel G. Morgan‡
NASA Ames Research Center,
Moffett Field, California 94035-1000

Introduction

THE number of optical techniques that may potentially be used during a given wind-tunnel test is continually growing. These include parameter sensitive paints that are sensitive to temperature or pressure, several different types of off-body and on-body flow visualization techniques, optical angle of attack (AOA), optical measurement of model deformation, optical techniques for determining density or velocity, and spectroscopic techniques for determining various flowfield parameters. Often in the past the various optical techniques were developed independently of each other, with little or no consideration for other techniques that might also be used during a given test. Part of the justification for this approach was that

Received 12 June 1999; accepted for publication 21 July 1999.

*Research Scientist, MS 236. Senior Member AIAA.
†Research Scientist, 28 Research Drive. Member AIAA.
‡Aerospace Engineer. Member AIAA.